Electronic Supplementary Material (ESI) for Journal of Materials Chemistry A.

[Electronic Supplementary Information]

Cationic porous organic polymers as an excellent platform for highly efficient removal of pollutants from water

Xiaochen Shen,[a] Si Ma,[a] Hong Xia*,[b] Zhan Shi,[c] Ying Mu,[a] and Xiaoming Liu*[a]

[a] *State Key Laboratory for Supramolecular Structure and Materials, College of Chemistry, Jilin University, Changchun, 130012, P.R. China.*

[b] *State Key Laboratory on Integrated Optoelectronics, College of Electronic Science and Technology, Jilin University, Changchun 130012, P.R. China.*

[c] *State Key Laboratory of Inorganic Synthesis and Preparative Chemistry, Jilin University, Changchun, 130012, P.R. China.*

**Email: xm_liu@jlu.edu.cn; hxia@jlu.edu.cn*

Table of Content

Section 15. Reference

Section 1. General Procedures

^{1}H spectra were recorded on a Avance III-400 NMR spectrometer, where chemical shifts (δ in ppm) were determined with a residual proton of the solvent as standard. Solid-state ^{13}C CP/MAS NMR measurement was recorded using a Bruker AVANCE III 400 WB spectrometer at a MAS rate of 5 kHz and a CP contact time of 2 ms. Elemental analyses were carried out on an Elementar model vario EL cube analyzer. The infrared spectra were recorded from 400 to 4000 cm^{-1} on an Avatar FT-IR 360 spectrometer by using KBr pellets. UV/Vis spectra have been carried out on a Perkin Elmer Lambda 950 spectrophotometer within the wavelength range 200–700 nm. Field emission scanning electron microscopy was performed on a SU8020 model HITACHI microscope. Transmission electron microscopy was performed on a JEOL model JEM-2100 microscope. The sample was prepared by drop-casting a supersonic methanol suspension of polymer onto a copper grid. Powder X-ray diffraction data were recorded on a PANalytical BV Empyrean diffractometer diffractometer by depositing powder on glass substrate, from 2ϑ = 1.5° to 40° with 0.02° increment at 25 °C. Thermogravimetric analysis (TGA) was performed on a TA Q500 thermogravimeter by measuring the weight loss while heating at a rate of 10 °C min^{-1} from room temperature to 800 °C under nitrogen. Nitrogen sorption isotherms were measured at 77 K with a JW-BK 132F analyzer. Before measurement, the samples were degassed in vacuum at 120 °C for more than 10 h. The Brunauer-Emmett-Teller (BET) method was utilized to calculate the specific surface areas and pore volume. X-Ray photoelectron spectroscopy (XPS) was measured with an ESCALAB 250 spectrometer (Thermo Scientific, Waltham, MA) with monochromatic Al Kα radiation (1486.6 eV).

Section 2. Materials and Synthesis

Materials: The reactants used in the experiment were purchased from Energy Chemical unless otherwise stated. Deuterated solvents and n-Butyllithium solution in hexanes (1.6 M) were obtained from J&K Scientific. Formaldehyde dimethyl acetal (FDA), anhydrous $FeCl_3$ and 1,2-dichloroethane (DCE) were obtained from Aladdin. Other organic solvents for reactions were distilled over appropriate drying reagents under nitrogen. 4,5-dihydro-3H-dinaphtho [2,1-c:1',2'-e] azepine and 3,3'-bis (2-naphthyl)-2,2'-bis (bromomethyl)-1,1'-binaphthyl were prepared according to the literature procedure.[1]

Synthesis of monomer C-NSA$_{Naph}$@Br:[2]

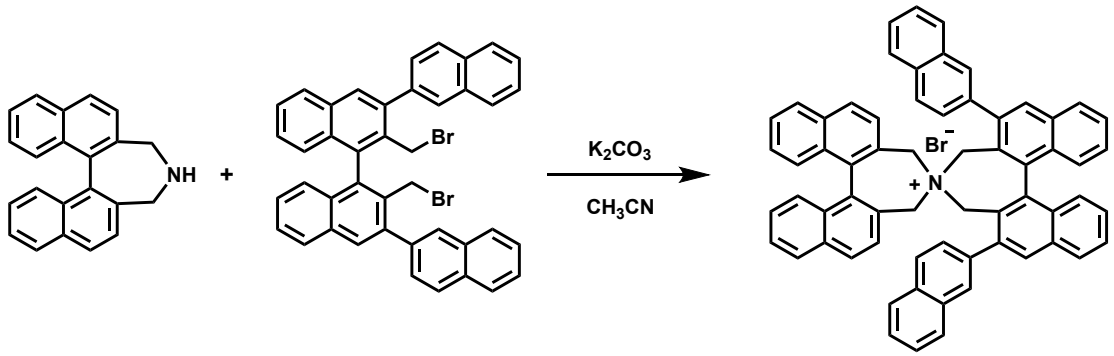

A mixture of 4,5-dihydro-3H-dinaphtho [2,1-c:1',2'-e]azepine (148 mg, 0.5 mmol), 3,3'-bis(2-naphthyl)-2,2'-bis(bromomethyl)-1,1'-binaphthyl (381 mg, 0.55 mmol) and K_2CO_3 (104 mg, 0.75 mmol) in dry acetonitrile (5.0 mL) was heated to reflux, and stirring was maintained for 10 h. The resulting mixture

was poured into water and extracted with CH_2Cl_2. The organic extracts were dried over Na_2SO_4 and concentrated. The residue was purified by column chromatography on silica gel (MeOH/CH_2Cl_2 = 1:30) to furnish monomer C-NSA$_{Naph}$@Br (345 mg, 0.38 mmol, 76% yield). ^{1}H NMR (400 MHz, $CDCl_3$): δ 8.47 (s, 3H, Ar-H), 8.13 (d, 5H, *J* = 8.0 Hz, Ar-H), 7.77 (t, 4H, *J* = 12.0 Hz, Np), 7.64 (t, 4H, *J* = 16.0 Hz, Ar-H), 7.31-7.40 (m, 8H, Np), 7.18 (d, 2H, *J* = 8.0 Hz, Ar-H), 7.07 (t, 2H, *J* = 16.0 Hz, Ar-H), 6.93 (d, 2H, *J* = 8.0 Hz, Ar-H), 6.01 (br, 4H, Np), 5.01 (br, 2H, Ar-CH_2), 4.42 (d, 2H, *J* = 16.0 Hz, Ar-CH_2), 4.15 (d, 2H, *J* = 12.0 Hz, Ar-CH_2), 3.60 (d, 2H, *J* = 12.0 Hz, Ar-CH_2) ppm; ^{13}C NMR (100 MHz, $CDCl_3$): δ 139.7, 139.6, 136.2, 134.3, 134.0, 133.5, 133.1, 131.0, 129.1, 128.9, 128.8, 128.7, 128.6, 128.3, 128.1,127.9, 127.8, 127.7, 127.6, 127.5, 127.1, 126.9, 125.0, 123.1, 62.5, 57.8 ppm.

Synthesis of cationic organic porous polymer C-NSA$_{Naph}$-HCP@Br:

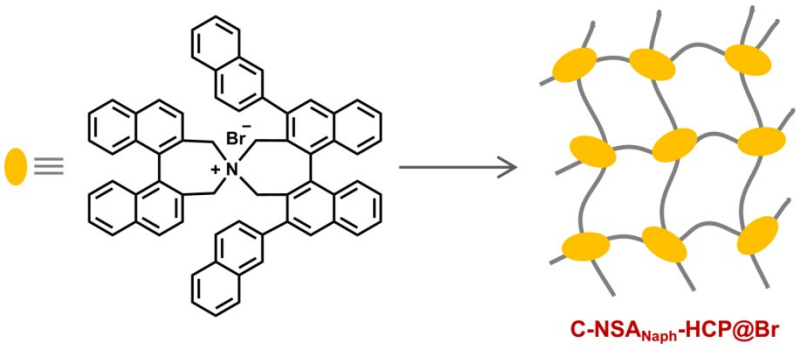

To the mixture of monomer C-NSA$_{Naph}$@Br (55.0 mg, 0.06 mmol) and anhydrous $FeCl_3$ (77.9 mg, 0.48 mmol) in 1,2-dichloroethane (2.0 mL), FDA (42.5 µL, 0.48 mmol) was added at room temperature. The mixture was heated to 80 °C and stirred for 24 h under a nitrogen atmosphere. The mixture was then cooled to room temperature, the precipitated network was filtered and washed with dichloromethane (10 mL × 3), methanol (10 mL × 3), and tetrahydrofuran (10 mL × 3), respectively. The product was then dispersed in 5 mL 1:1 H_2O/Methanol saturated solution of sodium bromide. After the mixture was stirred for 24 h at room temperature, the residue was filtered. Repeated the above step three times, the precipitate was washed with plenty of water. The further purification of the network was carried out by Soxhlet extraction from methanol and tetrahydrofuran for 24 h, respectively. The product was dried in vacuum for 24 h at 80 °C to give a brown powder C-NSA$_{Naph}$-HCP@Br (59.1 mg,

96.7% yield).

Section 3. IR Spectra

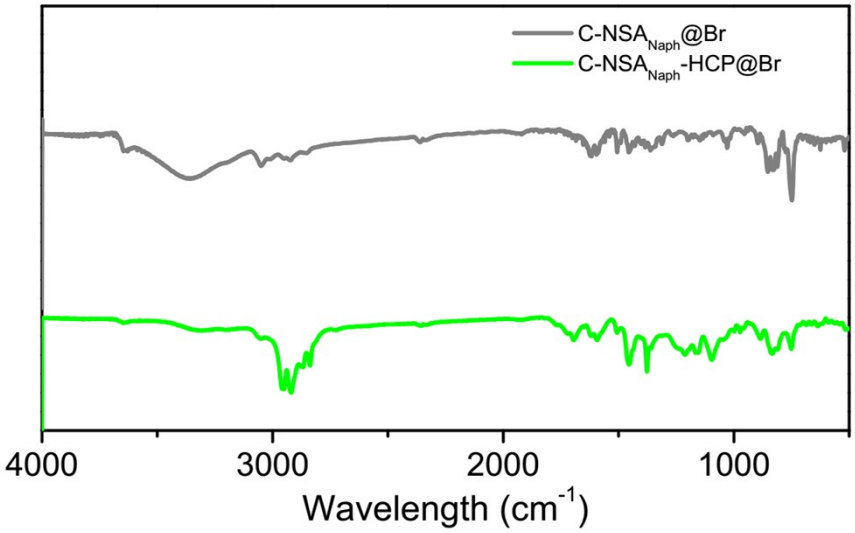

Figure S1. FT-IR spectra of N-spiroammonium salt monomers (C-NSA$_{Naph}$@Br) and its polymer (C-NSA$_{Naph}$-HCP@Br). The peaks at around 2930 cm^{-1} are originating from C-H stretching vibrations of –CH_2– groups.

Section 4. Solid State ^{13}C CP/MAS NMR

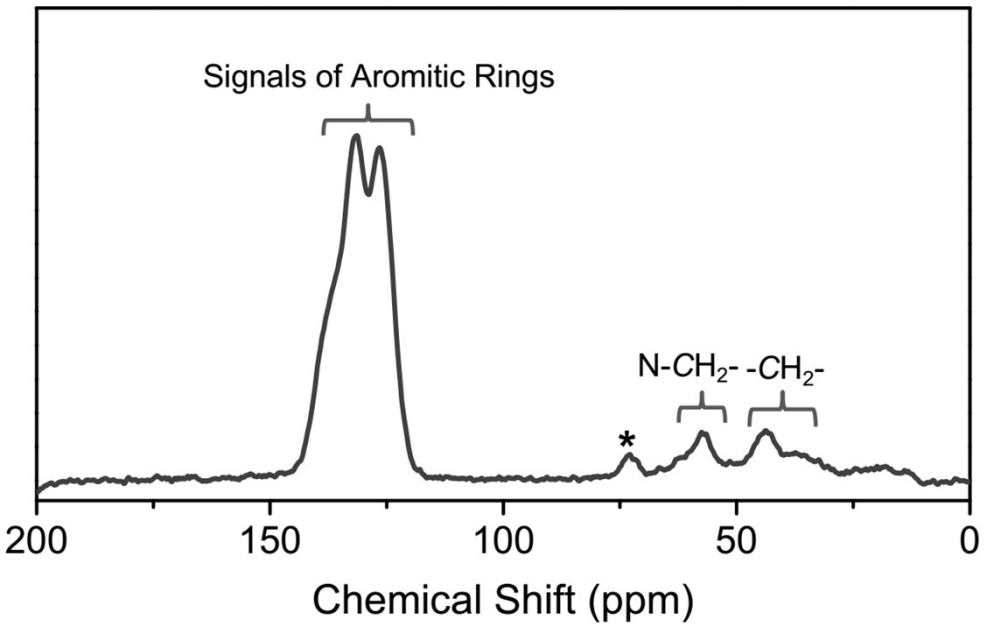

Figure S2. The solid-state ^{13}C-CP/MAS NMR spectrum of cationic porous organic polymer C-NSA$_{Naph}$-HCP@Br. The siganls from 120 to 145 ppm are assignable to aromatic carbon, and the weak peaks at about 58 and 42 ppm are attributed to the two types of methylene carbon in the polymer network.

Signal with * symbol is attributed to the carbon of -OCH_2- group in the polymer.[3]

Section 5. PXRD Spectrum

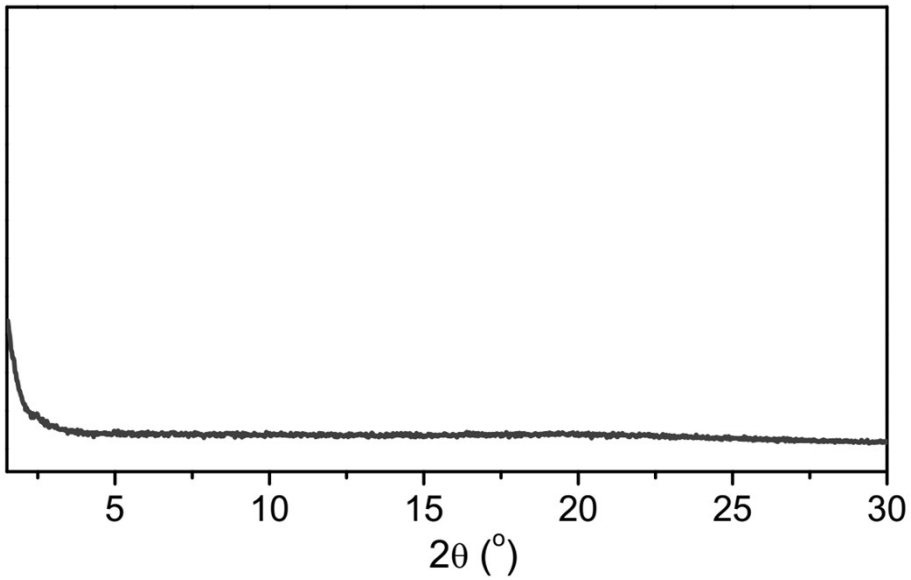

Figure S3. PXRD curve of cationic porous organic polymer C-NSA_{Naph}-HCP@Br.

Section 6. TGA Curve

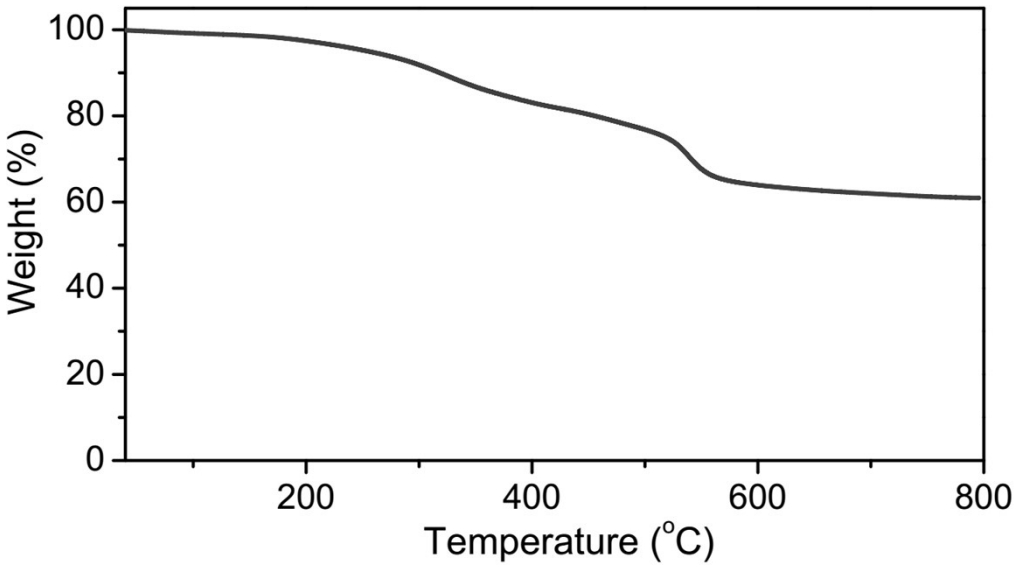

Figure S4. TGA curve of the cationic porous organic polymer C-NSA$_{Naph}$-HCP@Br.

Section 7. XPS Spectra

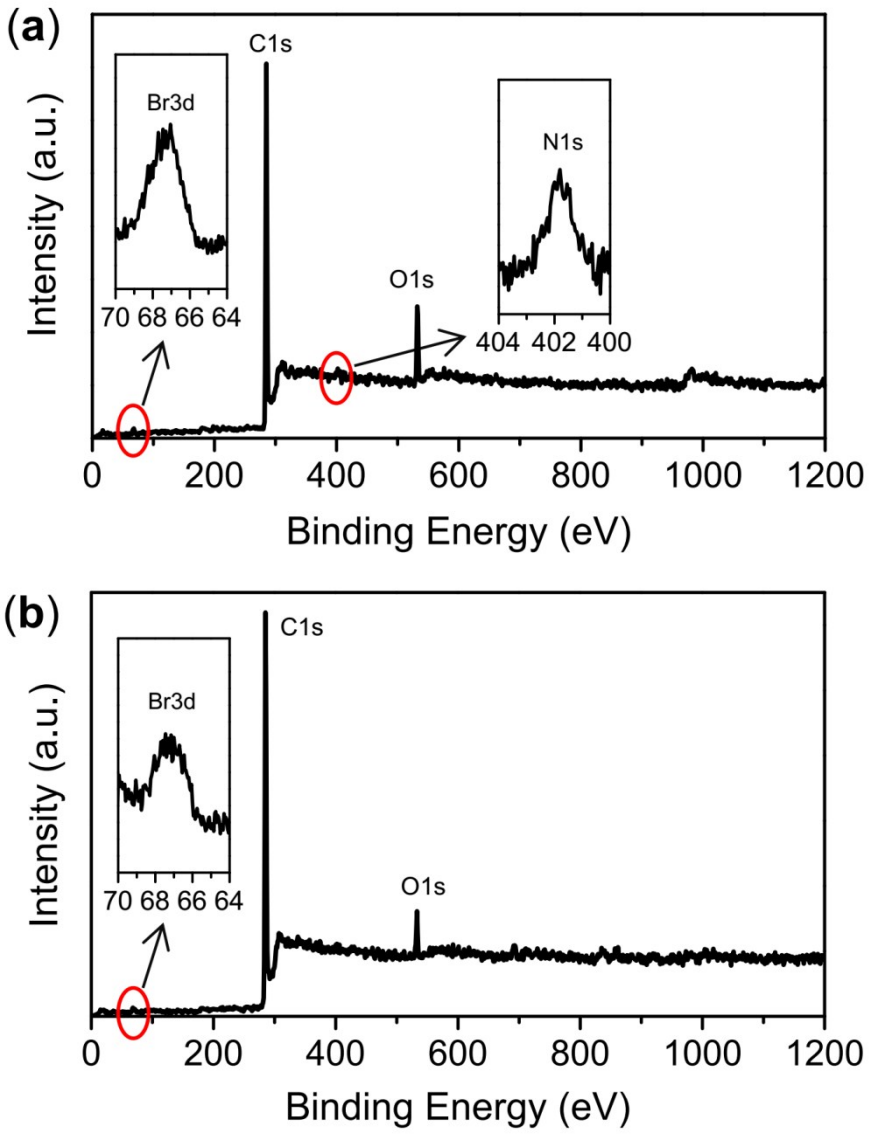

Figure S5. XPS patters of C-NSA$_{Naph}$@Br (a) and C-NSA$_{Naph}$-HCP@Br (b) recorded from 0 to 1200 eV.

Section 8. IR Spectra

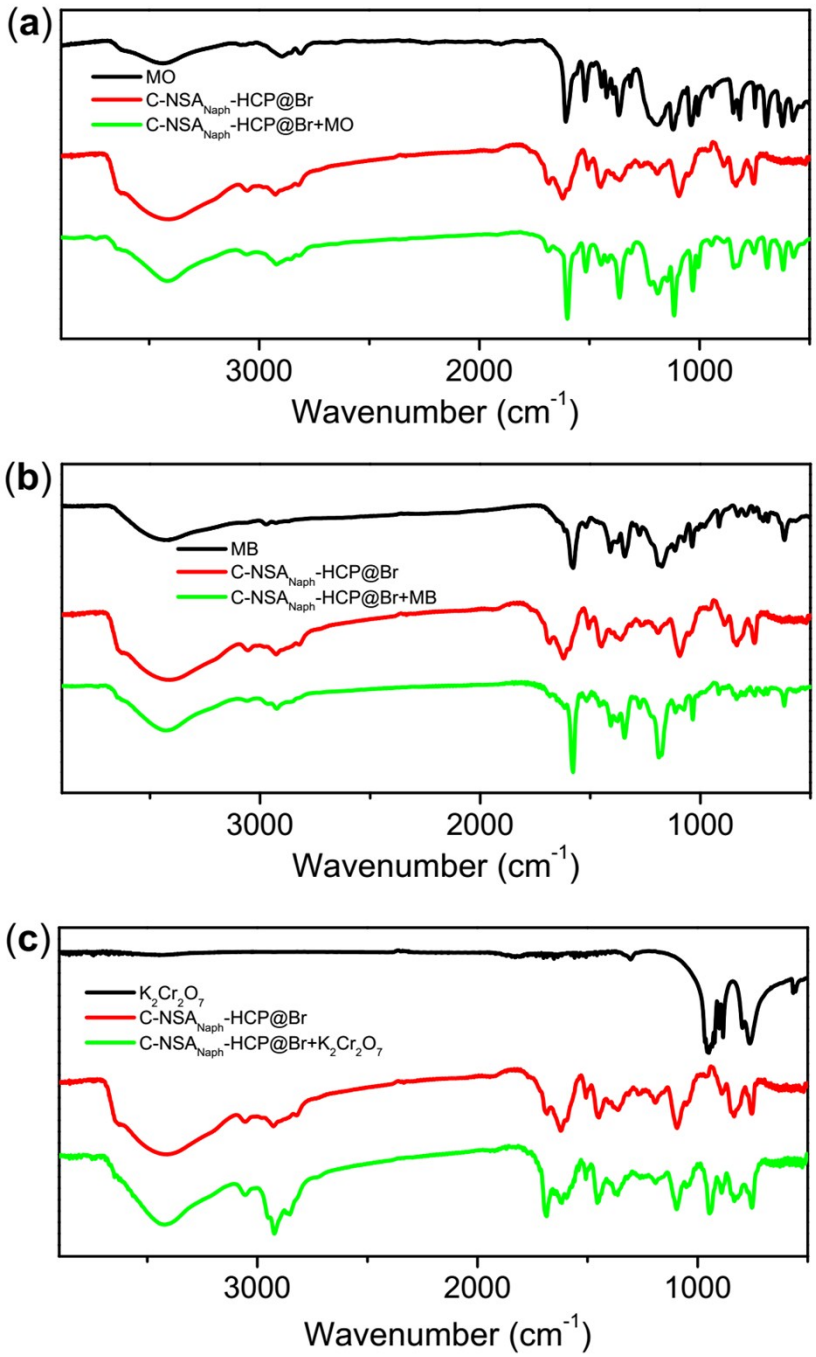

Figure S6. FT-IR spectra of pollutant, C-NSA$_{Naph}$-HCP@Br, and C-NSA$_{Naph}$-HCP@Br/pollutant.

Section 9. UV-vis Absorption Spectra

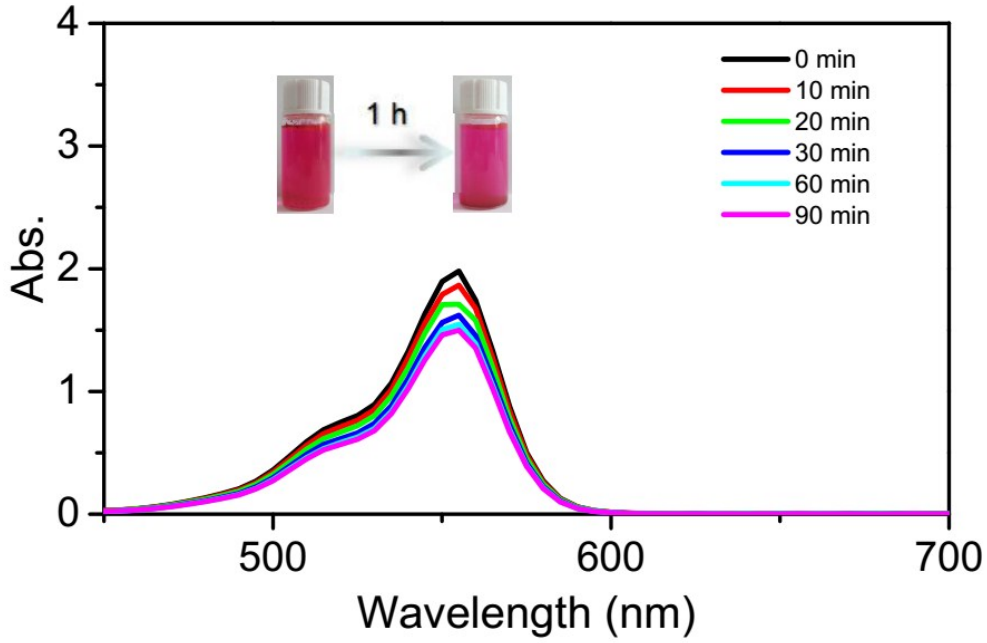

Figure S7. UV-vis absorption spectra of RB in water (c = 60 mg L^{-1}) at different times using C-NSA_{Naph}-HCP@Br (5.0 mg) as sorbent. The inset profiles display the change in color before and after adsorption.

Section 10. Sorption Kinetics

Table S1. A summary of the pseudo-second-order rate constant k_2 for different adsorption materials.[a]

Adsorbent	Mass (mg)	Methyl orange		k_2 (g mg^{-1} min^{-1})	Reference
		C (mg L^{-1})	V (mL)		
Si/Al-Fe	30	150	20	1.70×10^{-3}	*Appl. Surf. Sci.* **2013**, *280*, 726.
MWCNTs	15	40	50	2.31×10^{-3}	*Chem. Eng. J.* **2011**, *170*, 82.
PAC-HNO_3	100	500	50	5.17×10^{-4}	*Chemosphere* **2011**, *85*, 1269.
HJ-1	50	100	20	1.82×10^{-5}	*Colloids Surf. A* **2008**, *330*, 55.
Zn/Al-LDO	5	50	10	4.49×10^{-4}	*J. Colloid Interface Sci*. **2007**, *316*, 284.
PED-MIL-101	50	50	25	3.04×10^{-3}	*J. Hazard. Mater*. **2010**, *181*, 535.
MOF-235	5	40	50	9.10×10^{-4}	*J. Hazard. Mater*. **2011**, *185*, 507.
CNTs-A	30	150	40	2.00×10^{-3}	*ACS Appl. Mater. Interfaces* **2012**, *4*, 5749.
AHCP-1	5	20	5	1.07×10^{-3}	*Polym. Chem*. **2018**, Advance Article.
CMK-3	50	50	25	4×10^{-3}	*J. Colloid Interface Sci*. **2011**, 362, 457.
GO-CTS bead	5	30	10	8×10^{-4}	*ACS Appl. Mater. Interfaces* 2015, 7, 14439.
C-NSA_{Naph}-HCP@Br	**5**	**60**	**15**	**3.70×10^{-3}**	***This Work***

[a] Generally, the dye adsorption of adsorption materials conforms to the pseudo-second-order model. And we can evaluate the adsorption rate of different adsorbents through the value of pseudo-second-order rate constant k_2 in the same experimental conditions. Therefore, we found that C-NSA_{Naph}-HCP@Br has a faster adsorption rate.

Pseudo first order kinetic model

The linear form of pseudo first order kinetic model is expressed by the following equation:

$$\ln(Q_e - Q_t) = \ln Q_e - k_1 t$$

Where Q_t and Q_e are the amount of pollutants adsorbed at time *t* and equilibrium (mg g^{-1}), k_1 is the pseudo-first-order rate constant of adsorption process (min^{-1}).

The pseudo-second-order model

The linear form of pseudo second order kinetic model is expressed by the following equation:

$$\frac{t}{Q_t} = \frac{1}{k_2 Q_e^2} + \frac{t}{Q_e}$$

Where Q_t and Q_e are the amount of pollutants adsorbed at time *t* and equilibrium (mg g^{-1}), k_2 is the pseudo-second-order rate constant of adsorption process (g mg^{-1} min^{-1}).

Table S2. Parameters of the different adsorption kinetic models extracted from experimental adsorption data for C-NSA_{Naph}-HCP@Br.

Pollutants	Pseudo-first-order			Pseudo-second-order		
	k_1 (min^{-1})	Q_e (mg g^{-1})	R^2	k_2 (g mg^{-1} min^{-1})	Q_e (mg g^{-1})	R^2
MO	0.02576	55.20	0.844	3.70×10^{-3}	121.51	0.999
MB	0.02973	64.45	0.940	2.47×10^{-3}	116.69	0.998
RB	0.03046	23.77	0.987	4.06×10^{-3}	30.60	0.991
$K_2Cr_2O_7$	0.0264	63.80	0.990	2.62×10^{-3}	119.05	0.998

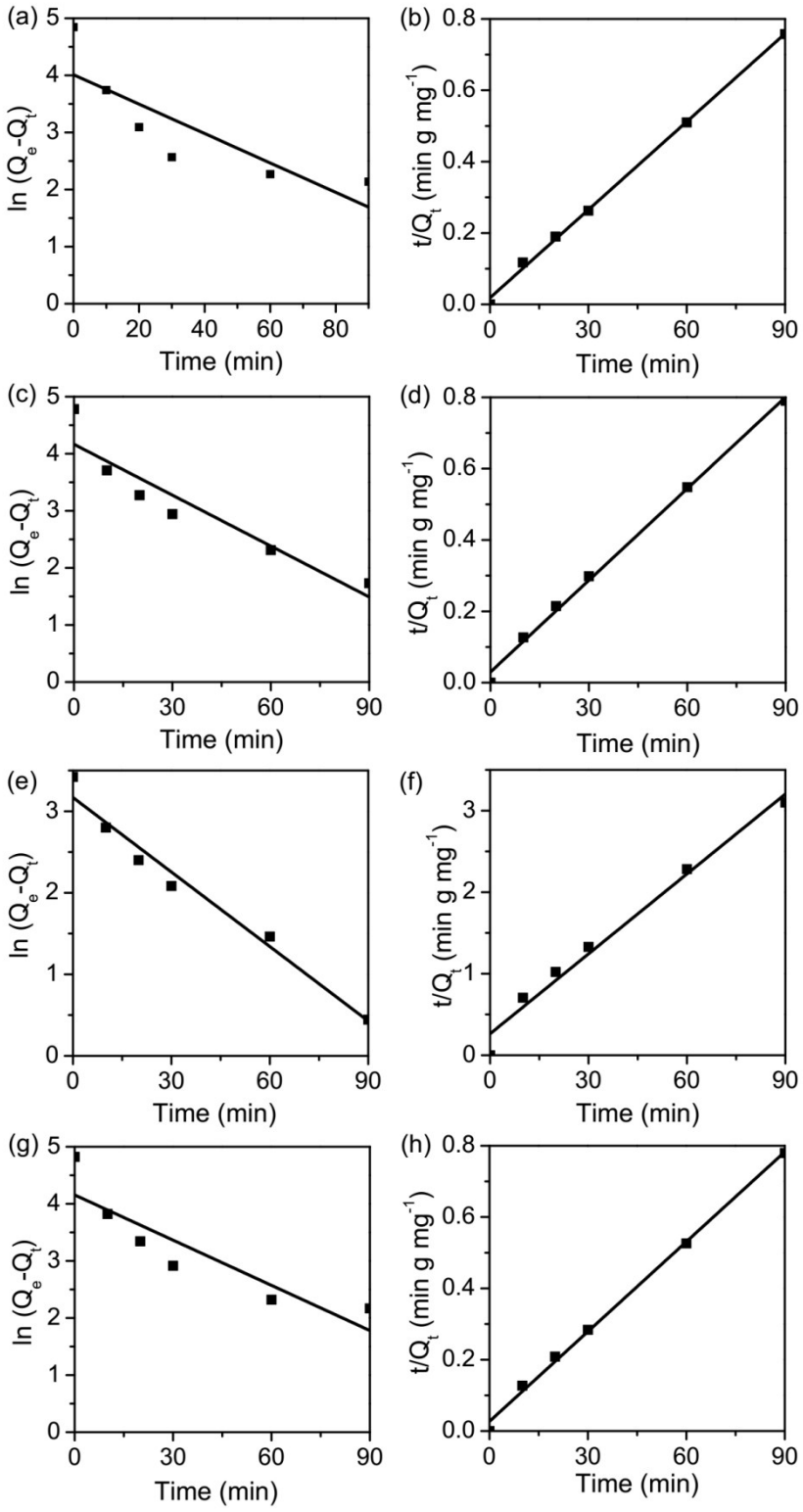

Figure S8. The pseudo-first-order model of MO (a), MB (c), RB (e), $Cr_2O_7^{2-}$ (g) and the pseudo-second-order model of 60 mg L^{-1} MO (b), MB (d), RB (f), $K_2Cr_2O_7$ (h). (C-NSANaph-HCP@Br, 5.0 mg; C = 60 mg L^{-1})

Section 14. Adsorption Capacity

Table S3. Adsorption capacities of methyl orange for the reported MOFs and porous silicon materials under different pH.

Adsorbent	**SA** ($m^2\ g^{-1}$)	**Condition**				**Reference**
		pH=1	pH=4	pH=10	pH=14	
C-NSA$_{Naph}$-HCP@Br	**788**	**99%**	**99%**	**93%**	**86%**	***This Work***
Metal-Organic Frameworks						
PED-MIL-101	3296		80%			*J. Hazard. Mater.* **2010**, *181*, 535.
UiO-66	1276		90%	28%		*Appl. Surf. Sci.* **2018**, *445*, 424.
NDA88-Cu	370		52%	68%		*J. Clean. Prod.* **2018**, *184*, 949.
MFC-O	782		98%	25%		*Chemoshere* **2018**, *199*, 435.
TPN/MNPs	No description		99%	89%	8%	*J. Iranian Chem. Soc.* **2018**, *15*, 733.
55% SA-MIL-101	1387		97%	10%		*RSC Adv.* **2018**, *8*, 20517.
$[Cd(INA)_2 \cdot (H_2O)]$.ISB	384		17%	16%		*J. Solid State Chem.* **2017**, *255*, 157.
MOR-1–HA	1182	87%	96%			*ChemPlusChem* **2017**, *82*, 1188.
MIL-68(Al)	1346	destroy	98%	98%	destroy	*Water Sci. Technol.* **2017**, *75*, 2800.

PCN-222	2336		43%	30%		*RSC Adv.* **2017**, *7*, 16273.
Porous Silicons						
Si/Al-Fe	243	32%	70%	32%	13%	*Appl. Surf. Sci*. **2013**, *280*, 726.
SAPAS@MnNP	85	32%	75%	85%		*J. Colloid Interface Sci*. **2016**, *483*, 118.
CPMO-0T	10		85%	63%		*J. Mater. Chem. A* **2016**, *4*, 17866.
Mg-Al LDH	No description		98%	41%		*J. Chem. Eng. Data* **2011**, *56*, 4217.
Other Adsorbents						
TiO_2@GAC	No description	96%	87%	75%		*Sci Rep*. **2018**, *8*, 6463.
mesoporous TiO_2	161		87 %	78 %		*J. Hazard. Mater.* **2010**, *181*, 204.
CNTs-A	535		81%	81%		*ACS Appl. Mater. Interfaces* **2012**, *4*, 5749.
NH_2-MWCNTs	160	72%	58%	26%		*RSC Adv*. **2014**, *4*, 55162.
Core–shell Cu@Cu_2O	No description	88%		<1 %		*Chem. Eng. J*. **2013**, *223*, 76.
H-δ-MnO_2	92		34%	8%		*J. Mater. Chem. A* **2015**, *3*, 5674.

Section 11. Adsorption isotherm models

The Langmuir isotherm model:

$$Q_e = \frac{Q_m k_L C_e}{1 + k_L C_e}$$

The Feundlich isotherm model:

$$Q_e = k_F C_e^{\frac{1}{n}}$$

Where k_L (mg^{-1}) and Q_m ($mg\ g^{-1}$) are the Langmuir isotherm constants; k_F (mg^{-1}) and n are the Feundlich isotherm constants; C_e are the concentration at equilibrium ($mg\ L^{-1}$), Q_e are the amount of fluoride adsorbed at equilibrium ($mg\ g^{-1}$).

Table S4. Parameters of the different isotherm models extracted from experimental adsorption isotherms data for C-NSA_{Naph}-HCP@Br.

Pollutants	Langmuir isotherm			Freundlich isotherm		
	Q_m ($mg\ g^{-1}$)	k_L (mg^{-1})	R^2	k_F (mg^{-1})	n	R^2
MO	1009.73	0.25477	0.990	388.79	4.99	0.873
MB	823.30	0.07972	0.995	233.03	4.28	0.884
RB	141.75	0.01457	0.937	23.92	3.67	0.972

$K_2Cr_2O_7$	744.98	0.2053	0.985	302.00	5.73	0.890

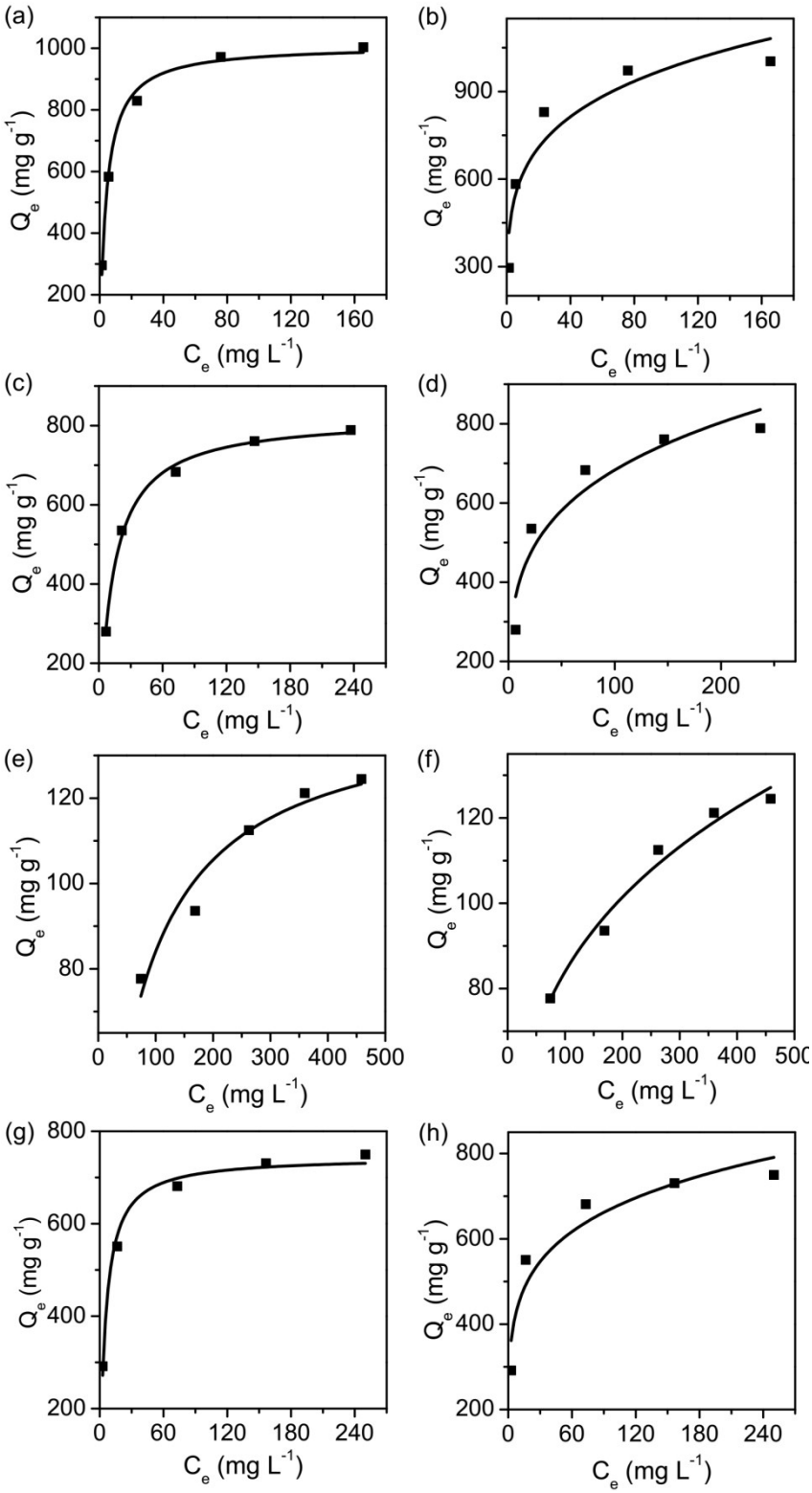

Figure S9. Adsorption isotherm of MO, MB, RB, $Cr_2O_7^{2-}$ Langmuir line (a, c, e and g) and Freündlich line (b, d, f, and h) respectively.

Section 12. UV-vis Absorption Spectra

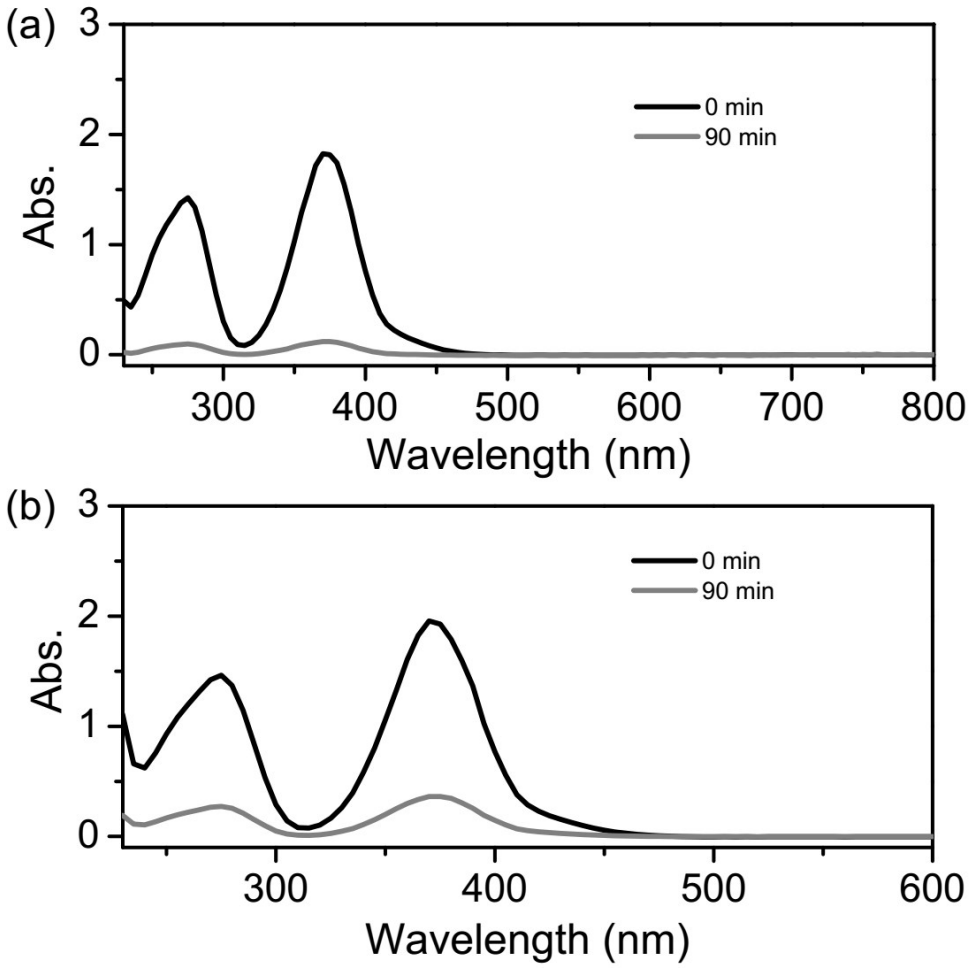

Figure S10. (a) Time-dependent UV-vis absorption spectra of $Cr_2O_7^{2-}$ together with 1-fold of disturbing ions in the presence of C-NSA_{Naph}-HCP@Br. (b) Time-dependent UV-vis absorption spectra of $Cr_2O_7^{2-}$ together with 5-fold of disturbing ions in the presence of C-NSA_{Naph}-HCP@Br.

Section 13. IR and ^{13}C NMR Spectra

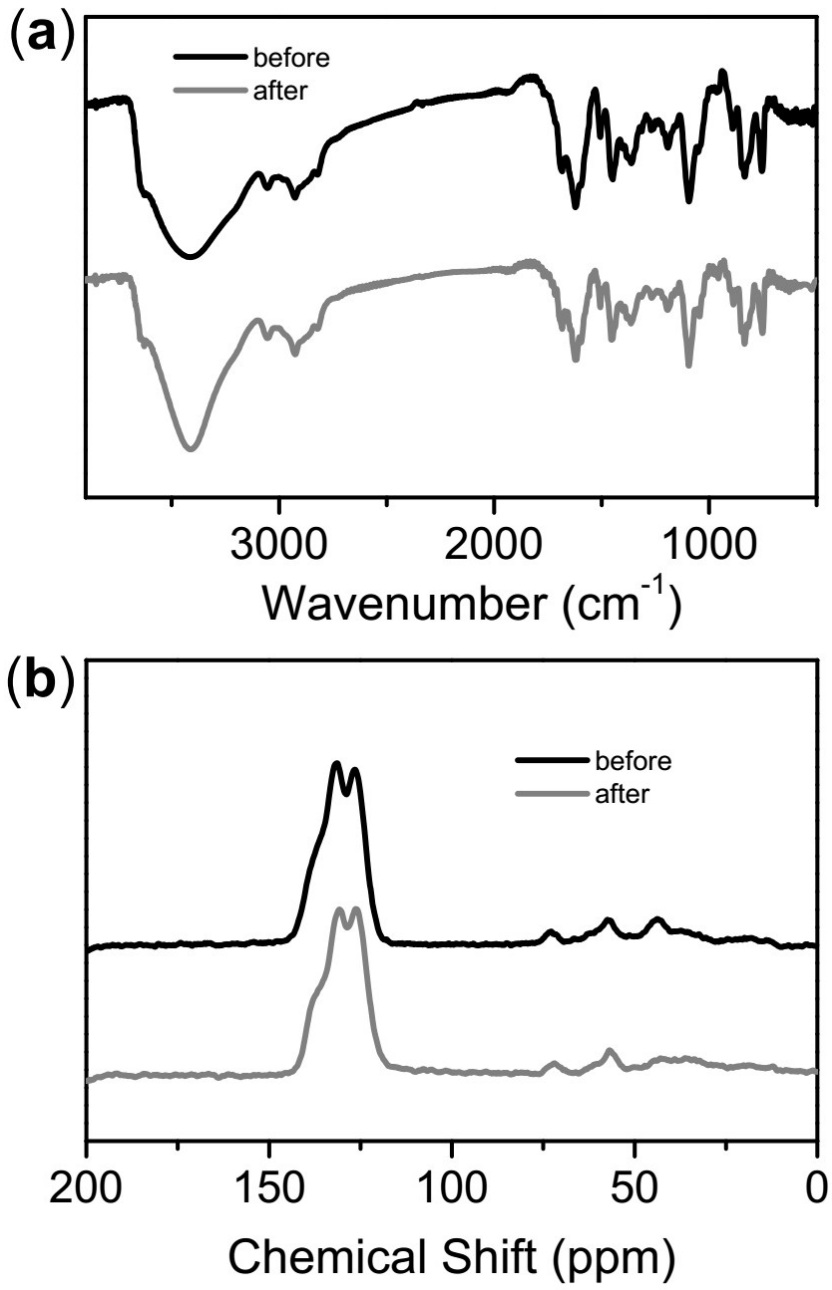

Figure S11. FT-IR spectra (a) and ^{13}C CP/MAS NMR spectra (b) of C-NSA$_{Naph}$-HCP@Br before (black line) and after the sixth run (gray line).

Section 14. Adsorption Capacity

Table S5. Adsorption capacities of dichromate anion for the reported materials.

Adsorbent	**SA** ($m^2\ g^{-1}$)	**Q_{max}** ($mg\ g^{-1}$)	**Recycling**	**Reference**
Metal-Organic Frameworks				
FIR-54	No description	103	5	*Chem. Mater.* **2015**, *27*, 205.
1-Br	No description	128	No description	*Chem. Commun.* **2017**, *53*, 1860.
TMU-3	No description	145	No description	*Inorg. Chem.* **2016**, *55*, 5507.
1-SO_4	No description	166	No description	*Angew. Chem., Int. Ed.* **2016**, *55*, 7811.
MOR-2	354	194	10	*J. Mater. Chem. A*, **2017**, *5*, 14707.
SC–SC	No description	207	No description	*Chem. Commun.* **2017**, *53*, 9206.
MONT-1	No description	212	5	*RSC Adv.* **2016**, *6*, 33888.
ABT 2ClO_4	No description	214	No description	*Angew. Chem. Int. Ed.* **2013**, *52*, 13769.
MOR-1–HA	1004	240	No description	*Chem. Sci.* **2016**, *7*, 2427.
ZJU-101	561	245	No description	*Chem. Commun.* **2015**, *51*, 14732.
UiO-66-NH_2@silica	730	277	No description	*J. Mater. Chem. A*, **2018**, *6*, 2742.

$[Cu_2L(H_2O)_2(NO_3)_2$·5.5H2O	No description	223	No description	*Chem. Eur. J.*, **2018**, *24*, 2718.
Porous Organic Polymers				
POP-Im1	negligible	172	No description	*ACS Appl. Mater. Interfaces*. **2016**, *8*, 18904.
PANI/H-TNBs	No description	157	10	*Polym. Chem.* **2016**, *7*, 785.
DEX-Cr	No description	248	No description	*Environ. Prog. Sus. Energy.* **2015**, 34, 387.
C-NSA$_{Naph}$-HCP@Br	**788**	**745**	**6**	***This Work***
Activated Carbons				
ACF	1565	116	No description	*Ind. Eng. Chem. Res.* **2005**, *44*, 1027.
PANI–Fe/OMC	56	172	No description	*RSC Adv.*, **2014**, *4*, 58362.
Acticarbone	1210	186	No description	*J. Hazard. Mater.* **2005**, *123*, 223.
Fe/CMK-3	679	257	7	*Chem. Eng. J*. **2014**, *239*, 114.
Activated carbons (CKW)	1255	316	No description	*J. Hazard. Mater.* **2005**, *123*, 223.
PAC	2402	390	No description	*Water Res.* **1995**, *29*, 2174.
Waste slurry	No description	640	10	*Water Res.* **1989**, *23*, 1161.
Mesoporous Silicons				
NN-sicilia	55	119	No description	*J. Colloid Interface Sci.* **2008**, *318*, 309

NNN-SBA-1	126	211	No description	*Chem. Mater.* **2002**, *14*, 4603.
Other Adsorbents				
Mesoporous TiO_2	161	34	5	*J. Hazard. Mater.* **2010**, *181*, 204.
Bagasse fly ash	440	259	No description	Environmentalist, **1999**, *19*, 129.
biofilm on nZVI-C-A beads	No description	474	No description	*Ind. Eng. Chem. Res.* **2016**, *55*, 5973
Polyethyleneimine and graphene oxide composite	No description	540	5	*J. Mater. Chem. A.* **2014**, *2*, 12561.

Section 15. Reference

[1] J. M. Hawkins, G. C. Fu, *J. Org. Chem.,* 1986, **51**, 2820.

[2] T. Ooi, M. Kameda, K. Maruoka, *J. Am. Chem. Soc.,* 2003, **125**, 5139.

[3] (a) X. Zhu, S. Mahurin, S. An, C. Do-Thanh, C. Tian, Y. Li, L. Gill, E. Hagaman, Z. Bian, J. Zhou, J. Hu, H. Liu, S. Dai, *Chem. Commun.,* 2014, **50**, 7933; (b) B. Li, R. Gong, W. Wang, X. Huang, W. Zhang, H. Li, C. Hu, B. Tan, *Macromolecules,* 2011, **44**, 2410.